The N- or C-terminal cytoplasmic regions of P4-ATPases determine their cellular localization

Sayuri Okamoto[a,†], Tomoki Naito[a,†,‡], Ryo Shigetomi[a], Yusuke Kosugi[b], Kazuhisa Nakayama[a], Hiroyuki Takatsu[a], and Hye-Won Shin[a,*]

[a]Department of Physiological Chemistry, Graduate School and [b]Faculty of Pharmaceutical Sciences, Kyoto University, Sakyo-ku, Kyoto 606-8501, Japan.

ABSTRACT **Mammalian P4-ATPases specifically localize to the plasma membrane and the membranes of intracellular compartments. P4-ATPases contain 10 transmembrane domains, and their N- and C-terminal (NT and CT) regions face the cytoplasm. Among the ATP10 and ATP11 proteins of P4-ATPases, ATP10A, ATP10D, ATP11A, and ATP11C localize to the plasma membrane, while ATP10B and ATP11B localize to late endosomes and early/recycling endosomes, respectively. We previously showed that the NT region of ATP9B is critical for its localization to the Golgi apparatus, while the CT regions of ATP11C isoforms are critical for Ca^{2}+-dependent endocytosis or polarized localization at the plasma membrane. Here, we conducted a comprehensive analysis of chimeric proteins and found that the NT region of ATP10 proteins and the CT region of ATP11 proteins are responsible for their specific subcellular localization. Importantly, the ATP10B NT and the ATP11B CT regions were found to harbor a trafficking and/or targeting signal that allows these P4-ATPases to localize to late endosomes and early/recycling endosomes, respectively. Moreover, dileucine residues in the NT region of ATP10B were required for its trafficking to endosomal compartments. These results suggest that the NT and CT sequences of P4-ATPases play a key role in their intracellular trafficking.**

Monitoring Editor
Thomas Martin
University of Wisconsin, Madison

Received: Apr 7, 2020
Revised: Jun 19, 2020
Accepted: Jun 25, 2020

INTRODUCTION

Cellular membranes exhibit transbilayer lipid asymmetry, which is regulated by lipid scramblases, floppases, and flippases (Coleman *et al.*, 2013; Murate *et al.*, 2015; Andersen *et al.*, 2016; Bevers and Williamson, 2016; Shin and Takatsu, 2019). The P4-ATPase family is a subfamily of the P-type ATPase superfamily that translocates lipids from the exoplasmic or luminal leaflet to the cytosolic leaflet of cellular membranes, while other P-type ATPases mostly transport cations to regulate cation gradients across membranes (Palmgren and Nissen, 2011; Andersen *et al.*, 2016; Palmgren *et al.*, 2019; Shin and Takatsu, 2019). Among P4-ATPases, ATP9A localizes to the *trans*-Golgi network (TGN) and endosomes, while ATP9B specifically localizes to the TGN (Takatsu *et al.*, 2011; Shin and Takatsu, 2019). ATP10A, ATP10D, ATP11A, and ATP11C localize to the plasma membrane and exhibit substrate specificity: phosphatidylcholine for ATP10A, glucosylceramide for ATP10D, and phosphatidylserine and phosphatidylethanolamine for ATP11A and ATP11C (Takatsu *et al.*, 2011, 2014; Naito *et al.*, 2015; Takada *et al.*, 2015; Roland *et al.*, 2019; Shin and Takatsu, 2019). ATP10B localizes to late endosomes, and ATP11B localizes to early/recycling endosomes (Takatsu *et al.*, 2011). ATP11B appears to translocate phosphatidylserine (Wang *et al.*, 2018). Although these P4-ATPases travel to cellular compartments via continuous intracellular trafficking pathways at the steady state as well as during biosynthesis, how they are able to localize to specific organelles is unknown

This article was published online ahead of print in MBoC in Press (http://www.molbiolcell.org/cgi/doi/10.1091/mbc.E20-04-0225) on July 2, 2020.

The authors declare no conflicts of interest.

†These authors contributed equally to this work.

‡Present address: Lee Kong Chian School of Medicine, Nanyang Technological University, 11 Mandalay Road, 308232, Singapore.

Author contributions: H.-W.S. conceived and designed the experiments. S.O., T.N., R.S., Y.K., and H.T. performed the experiments. S.O., T.N., H.T., and H.-W.S. analyzed the data. H.-W.S. wrote the manuscript. All authors discussed results and commented on the manuscript.

*Address correspondence to: Hye-Won Shin (shin@pharm.kyoto-u.ac.jp).

Abbreviations used: A domain, actuator domain; CT, C-terminal; EEA1, early endosome antigen 1; ER, endoplasmic reticulum; FRB, FK506 binding protein-rapamycin binding domain; GlcCer, glucosylceramide; Lamp-1, lysosomal-associated membrane protein; NT, N-terminal; NBD, nitrobenzoadiazol; N domain, nucleotide binding domain; PC, phosphatidylcholine; PI4P, phosphatidylinositol-4-phosphate; P domain, phosphorylation domain; TGN, *trans*-Golgi network; TfnR, transferrin receptor; WT, wild type.

(Bryde *et al.*, 2010; van der Velden *et al.*, 2010; Takatsu *et al.*, 2011; Steinberg *et al.*, 2013).

P4-ATPases are composed of 10 transmembrane domains and 3 cytoplasmic domains [N (nucleotide binding), P (phosphorylation), and A (actuator)], and their N- and C-termini both face the cytosol (Hiraizumi *et al.*, 2019; Timcenko *et al.*, 2019). The C-terminal cytoplasmic region of Drs2p, a yeast P4-ATPase, acts as a regulatory domain that can autoinhibit the enzymatic activity by interacting with its N-domain (Natarajan *et al.*, 2009; Azouaoui *et al.*, 2017; Timcenko *et al.*, 2019). The C-terminal region of ATP8A2 also seems to act as an autoinhibitory domain, although its regulation is more complex (Chalat *et al.*, 2017). Moreover, the C-terminal region of ATP8A1 seems to bind to its N-domain in the E2P state (Hiraizumi *et al.*, 2019). Therefore, the C-terminal domains of P4-ATPases seem to play a role in their enzymatic activities.

On one hand, the N-terminus of ATP9B is required for its localization to the Golgi (Takatsu *et al.*, 2011). The C-terminus of the ATP11C-a isoform is critical for signal-driven endocytosis via phosphorylation, while the C-terminal region of the ATP11C-b isoform contains an LLSYKH sequence that allows its polarized localization at the plasma membrane (Takatsu *et al.*, 2017; Takayama *et al.*, 2019). Moreover, ATP13A2, a member of the P5-ATPase family, contains an NT hydrophobic extension that is critical for its lysosomal localization (Holemans *et al.*, 2015), and ATP7B, a member of the P1B-ATPase family, contains a dileucine motif in its C-terminal cytoplasmic region that is required for its trafficking between the TGN and the plasma membrane (Lalioti *et al.*, 2014). Therefore, the NT and CT regions of P4-ATPases appear to play important roles in their localization to specific subcellular compartments.

Here, we hypothesized that P4-ATPases contain intracellular trafficking and/or targeting signals in their N- or C-terminal cytoplasmic regions that control their localization. This hypothesis was examined using a series of chimeric ATP10 and ATP11 proteins.

RESULTS

The NT cytoplasmic regions of ATP10A, ATP10B, and ATP10D are responsible for their localization

To examine the importance of the N- and C-termini of the ATP10 proteins in their subcellular localization, we first established expression vectors of C-terminally hemagglutinin (HA)-tagged ATP10 chimeras in which the N-terminal (NT) or C-terminal (CT) regions were exchanged among ATP10A, ATP10B, and ATP10D (Supplemental Table 1). In B-ATP10A and D-ATP10A, the N-terminus of ATP10A was exchanged with that of ATP10B or ATP10D, respectively, while in ATP10A-B and ATP10A-D, the C-terminus of ATP10A was exchanged with that of ATP10B or ATP10D, respectively (Figure 1 and Supplemental Table 1). Cells were cotransfected with expression vectors for any of the chimeric constructs and N-terminally FLAG-tagged CDC50A, and the subcellular localization of the chimeras was

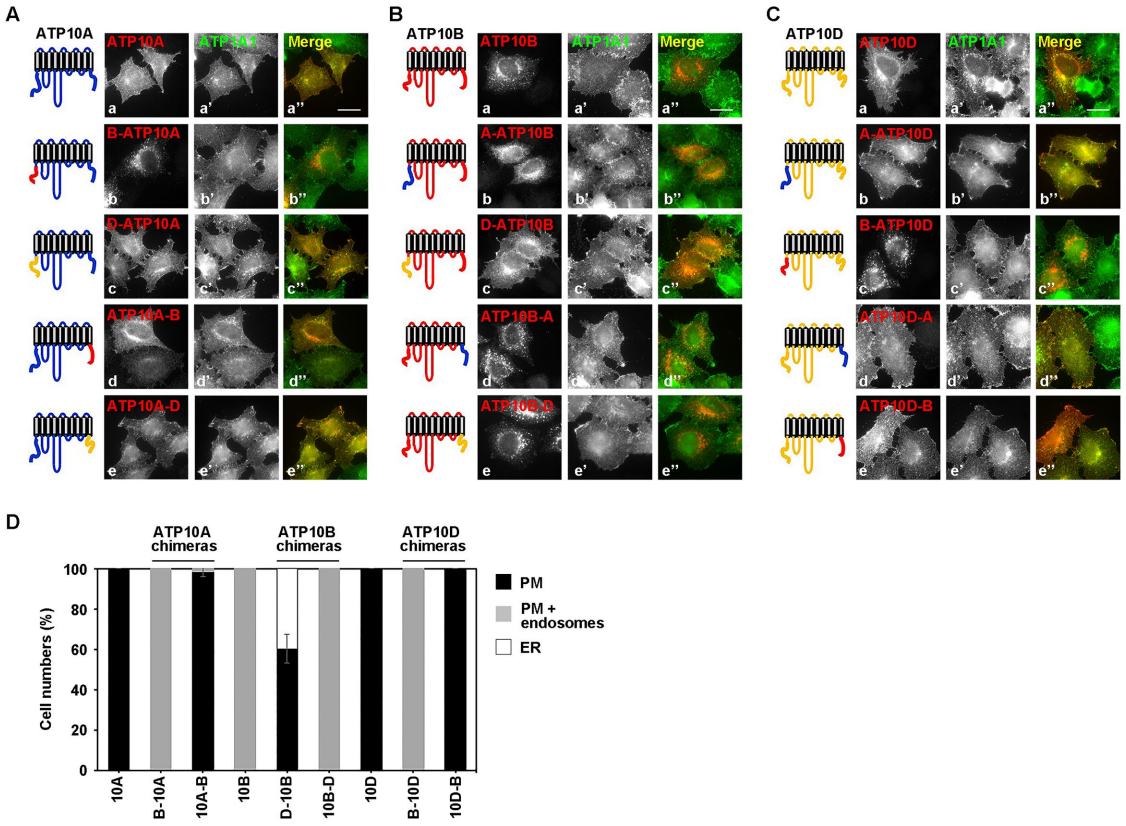

FIGURE 1: Cellular localization of ATP10 chimeric proteins. (A, B, C) HeLa cells transiently coexpressing N-terminally FLAG-tagged CDC50A and C-terminally HA-tagged ATP10A, ATP10B, ATP10D, or their N- or C-terminus–swapped mutants, were fixed and stained for HA and ATP1A1 (a plasma membrane marker) followed by incubation with a Cy3-conjugated anti-rat antibody and an Alexa Fluor 488–conjugated anti-rabbit secondary antibody. Scale bars, 20 μm. (D) HeLa cells expressing ATP10A, ATP10B, or ATP10D, or each of their chimeras, were grouped into three categories: cells in which all the chimeric protein localized to the plasma membrane (PM), cells in which the chimeric protein localized to the plasma membrane and endosomes (PM + endosomes), and cells in which the chimeric protein localized to the endoplasmic reticulum (ER). For each condition, 283–371 cells were counted. Graphs display the average ± SD of three independent experiments.

observed using the plasma membrane marker ATP1A1 (Figure 1). ATP10A and ATP10D localized to the plasma membrane, and ATP10B localized to late endosomes, consistent with our previous report (Figure 1, A–C, a–a″; Naito *et al.*, 2015). Notably, chimeras with exchanged NT region, B-ATP10A and B-ATP10D, were localized to endosomes (Figure 1A, b–b″, and C, c–c″), although a small amount of protein remained at the plasma membrane. On the other hand, D-ATP10B did not localize to late endosomes but instead appeared at the plasma membrane (Figure 1B, c–c″). Despite that B-10A and B-10D as well as ATP10B mostly appeared in endosomal structures, some proteins were observed in the plasma membrane probably because of intracellular trafficking in the biosynthetic pathways and/or in the steady state. Therefore, the quantitation of colocalization between the chimeras and a plasma membrane marker may not correctly exhibit the extent of each chimera's translocation from the plasma membrane to endosomes. And thus, the numbers of cells in which the chimera localized to the plasma membrane only, to the plasma membrane and endosomes, or to the endoplasmic reticulum (ER) were counted for each chimera (Figure 1D). B-ATP10A and B-ATP10D, which contained the N-terminus of ATP10B, became localized to endosomes, while D-ATP10B, which contained the N-terminus of ATP10D, became localized to the plasma membrane, although some remained in the ER. The A-ATP10B chimera localized to the ER, suggesting that it may not be folded properly (Figure 1B, b–b″). These results suggest that the N-termini of ATP10 proteins are critical for their subcellular localization.

In contrast to chimeras with exchanged NT region, no change in the localization of ATP10 proteins was observed when the CT regions were exchanged. ATP10A-B and ATP10D-B localized to the plasma membrane, similarly to wild-type (WT) ATP10A and ATP10D (Figure 1A, d–d″, C, e–e″, and D), and ATP10B-A and ATP10B-D localized to endosomes, similarly to WT ATP10B (Figure 1B, d–e″ and D). D-ATP10A, ATP10A-D, A-ATP10D, and ATP10D-A also localized to the plasma membrane, similarly to WT ATP10A and ATP10D (Figure 1A, c–c″ and e–e″, and C, b–b″ and d–d″).

We then asked whether B-ATP10A and B-ATP10D localized to late endosomes like WT ATP10B. As shown in Figure 2, B-ATP10A, B-ATP10D, and ATP10B colocalized with the late endosomal marker lysosomal-associated membrane protein (Lamp-1; Figure 2, A–C, c–c‴), but not with the early/recycling endosomal markers early endosome antigen 1 (EEA1) and transferrin receptor (TfnR; Figure 2, A–C, a–b‴). These results strongly suggest that the subcellular localization of the ATP10 proteins is determined by their NT regions.

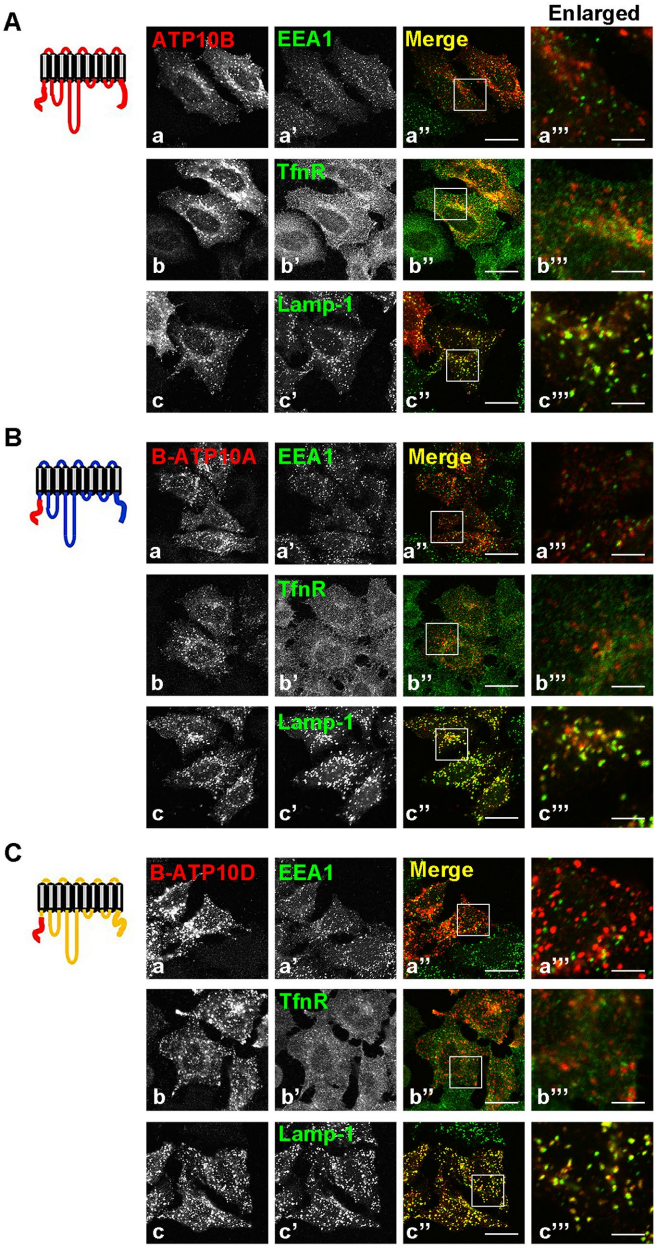

FIGURE 2: Endosomal localization of the N-terminus–swapped ATP10 chimeras. (A–C) HeLa cells transiently coexpressing C-terminally HA-tagged ATP10B, B-ATP10A, or B-ATP10D, and N-terminally FLAG-tagged CDC50A, were fixed and stained for HA and EEA1 (a marker for early endosome), TfnR (transferrin receptor, a marker for early/recycling endosomes), or Lamp-1 (a marker for late endosomes), followed by incubation with Cy3-conjugated anti-rat and Alexa Fluor 488–conjugated anti-mouse secondary antibodies. Images were taken by confocal microscopy. Scale bars, 20 μm. Scale bars in enlarged images, 5 μm.

Swapping the N- or C-termini did not affect the flippase activity of ATP10A and ATP10D

We previously showed that ATP10A and ATP10D specifically flip nitrobenzoxadiazole-labeled phosphatidylcholine (NBD-PC) and glucosylceramide (NBD-GlcCer), respectively (Naito *et al.*, 2015; Roland *et al.*, 2019). We asked whether swapping the N- or C-termini of ATP10 proteins altered their flippase activity. To this end, cells transiently cotransfected with expression vectors for any of HA-tagged ATP10 chimeras and FLAG-CDC50A were subjected to cell-based flippase assays with NBD-PC and NBD-GlcCer as substrates. The ability of each ATP10A chimera to translocate NBD-PC was comparable to that of WT ATP10A (Figure 3A). The ability of the ATP10D chimeras to translocate NBD-GlcCer was also largely unaffected but slightly lower than that of WT ATP10D (Figure 3B). The reduced activity of A-ATP10D compared with WT ATP10D (Figure 3B) was likely due to its lower expression level (Figure 3C). On one hand, the translocating activities of the ATP10D-A and ATP10D-B chimeras were supposed to be higher than WT ATP10D because the expression levels of the chimeras were much lower than that of WT ATP10D (Figure 3C). These results suggest that the chimeras retained the ability to translocate lipid substrates, although the increase of the flipping activity in cells expressing ATP10D-A and ATP10D-B is currently unclear. One possibility would be that the expression levels of the chimeras on the cell surface might be comparable to WT ATP10D. As a negative control, cells expressing ATPase-deficient mutants (ATP10A[EQ] and ATP10D[EQ]; Naito *et al.*, 2015; Roland *et al.*, 2019)

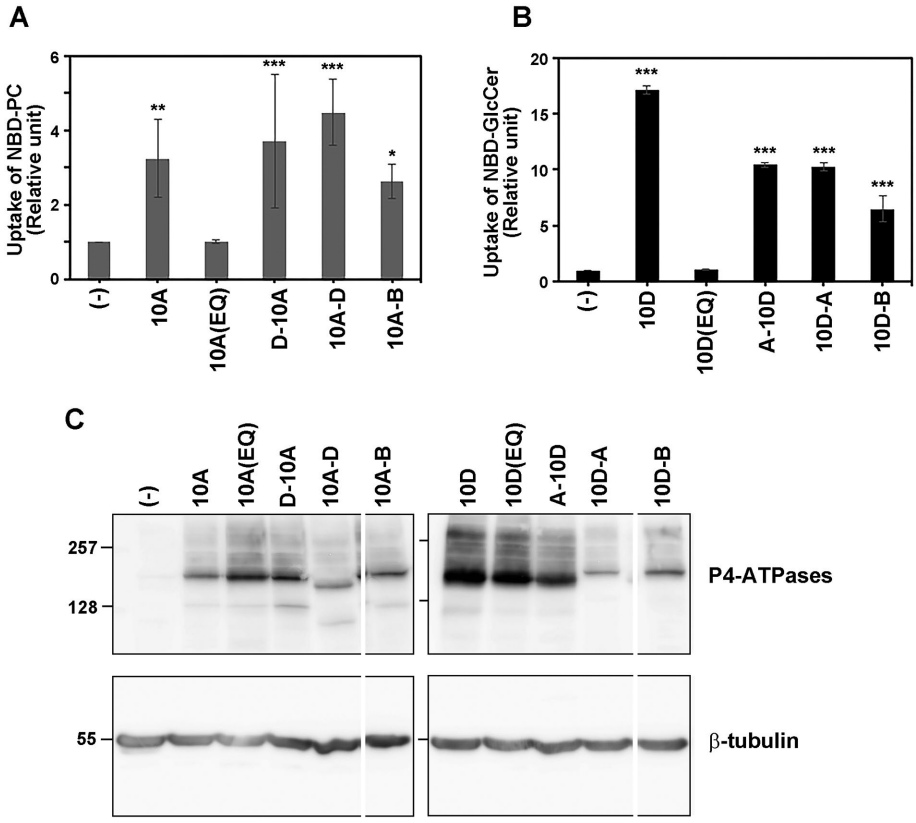

FIGURE 3: The lipid-transporting activity of chimeric proteins. (A, B, C) HeLa cells were transiently transfected with expression vectors for FLAG-tagged CDC50A and HA-tagged ATP10A, ATP10D, ATP10A(EQ), ATP10D(EQ), or each chimeric construct. The cells were washed with flippase assay buffer and incubated for 15 min at 15°C with NBD-PC (A) or NBD-GlcCer (B). After extraction with fatty acid–free BSA, the residual fluorescence intensity associated with the cells was determined by flow cytometry. The uptake of NBD-tagged lipids is shown relative to that in control HeLa cells (–). Graphs ± SD display the average from four (A) or three (B) independent experiments. Variance was assessed by comparison to control cells (–) using Student's *t* tests. *, $p < 0.05$; **, $p < 0.01$; ***, $p < 0.001$. (C) The cells were lysed and subjected to immunoblotting using anti-HA or anti–β-tubulin as an internal control.

did not show any flippase activity (Figure 3, A and B). Therefore, swapping the N- or C-termini among ATP10 proteins did not significantly affect their enzymatic activities.

The C-terminal cytoplasmic regions are responsible for the localization of ATP11A, ATP11B, and ATP11C

We next established expression vectors of C-terminally HA-tagged ATP11 chimeras in which the NT or CT regions were exchanged among ATP11A, ATP11B, and ATP11C. Cells were cotransfected with expression vectors for any of the chimeric constructs and FLAG-CDC50A, and the subcellular localization of the chimeras was visualized using the plasma membrane marker ATP1A1 (Figure 4). ATP11A and ATP11C localized to the plasma membrane, and ATP11B localized to early/recycling endosomes, as previously observed (Figure 4, A–C, a–a″; Takatsu *et al.*, 2011; Tone *et al.*, 2020). Chimeras with exchanged NT region, B-ATP11A and B-ATP11C, remained localized to the plasma membrane, similarly to WT ATP11A and ATP11C (Figure 4A, a–b″, and C, a–a″ and c–c″). Moreover, A-ATP11B and C-ATP11B remained localized to endosomes, similarly to WT ATP11B (Figure 4B, a–b″). By contrast, chimeras with exchanged CT region, ATP11A-B and ATP11C-B, were localized to endosomes (Figure 4A, d–d″, and C, e–e″), although some protein remained at the plasma membrane. Moreover, ATP11B-A and ATP11B-C were not localized to early/recycling endosomes but instead were observed at the plasma membrane (Figure 4B, d–e″). The numbers of cells in which the chimera localized to the plasma membrane, or to both the plasma membrane and endosomes, were counted (Figure 4D). ATP11A-B and ATP11C-B, which contain the C-terminus of ATP11B, became localized to endosomes, while ATP11B-A and ATP11B-C, which contain the C-termini of ATP11A and ATP11C, respectively, became localized to the plasma membrane and not to endosomes. These results suggest that the C-termini of ATP11 proteins are critical for their subcellular localization. Because both ATP11A and ATP11C localized to the plasma membrane, C-ATP11A, ATP11A-C, A-ATP11C, and ATP11C-A also localized to the plasma membrane (Figure 4A, c–c″ and e–e″, and C, b–b″ and d–d″). Because both ATP11A and ATP11C translocate NBD-PS and NBD-PE (Takatsu *et al.*, 2014), and ATP11A-C, like ATP11A, translocates both substrates (Takatsu *et al.*, 2017), swapping the C-termini among ATP11 proteins may not affect their enzymatic activity.

We then asked whether ATP11A-B and ATP11C-B localized to early/recycling endosomes. As shown in Figure 5, ATP11A-B, ATP11C-B, and ATP11B colocalized with early/recycling endosomal markers (Figure. 5, A–C, a–b‴) but not with the late endosomal marker (Figure 5, A–C, c–c‴). These results strongly suggest that the subcellular localization of the ATP11 proteins is determined by their C-terminal regions.

The N-terminus of ATP10B and the C-terminus of ATP11B are sufficient to determine their endosomal localization

Next, we asked whether the N-terminus of ATP10B and the C-terminus of ATP11B are solely responsible for their subcellular localization. When the N-terminus of ATP10B and the C-terminus of ATP11B were expressed, they distributed in the cytosol (Supplemental Figure S1), suggesting that these domains cannot be recruited to endosomal membranes by direct interaction with the membranes. Next, chimeric proteins were constructed in which the NT regions of ATP10 and CT regions of ATP11 were fused to Lyn_{11}-EGFP (the N-terminal 11 amino acids of Lyn fused to EGFP; Figure 6A). Lyn_{11} contains a plasma membrane–targeting signal, and the original construct Lyn_{11}-EGFP-FRB (FK506 binding protein [FKBP]–rapamycin binding domain) localized to the plasma membrane but not to other intracellular compartments, as expected (Figure 6B; Komatsu *et al.*, 2010; Takatsu *et al.*, 2017; Takada *et al.*, 2018). By contrast, the NT region of ATP10B fused to Lyn_{11}-EGFP, and the CT region of ATP11B fused to Lyn_{11}-EGFP (Lyn_{11}-EGFP-ATP10B-NT and Lyn_{11}-EGFP-ATP11B-CT, respectively) localized to intracellular endosomal compartments (Figure 6C and D, b–b‴). All other constructs (Lyn_{11}-EGFP-ATP10A-NT, -ATP11A-CT, and -ATP11C-CT) remained at the plasma membrane (Figure 6C, a–a‴, and D, a–a‴ and c–c‴). Although a large proportion of Lyn_{11}-EGFP-ATP10D-NT remained

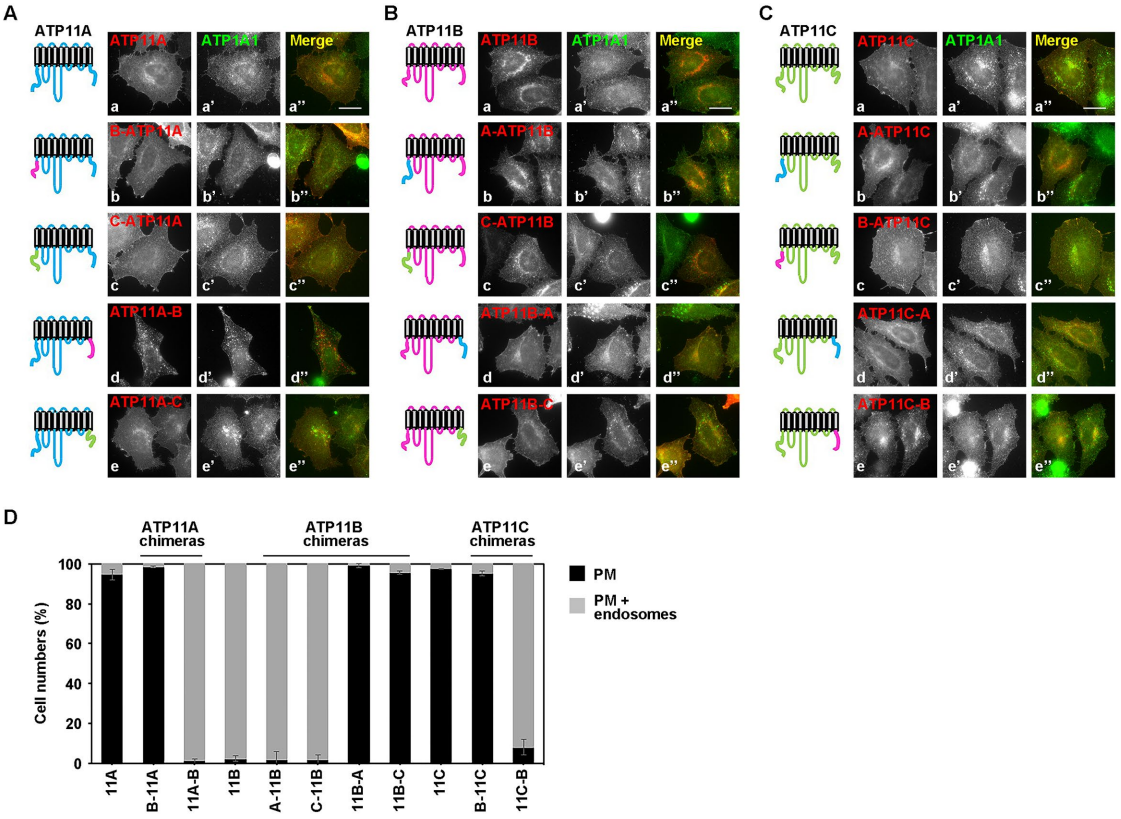

FIGURE 4: Cellular localization of ATP11 chimeric proteins. (A–C) HeLa cells transiently coexpressing N-terminally FLAG-tagged CDC50A and C-terminally HA-tagged ATP11A, ATP11B, ATP11C, or their N- or C-terminus–swapped mutants were fixed and stained for HA and ATP1A1 (a plasma membrane marker) followed by incubation with a Cy3-conjugated anti-rat antibody and an Alexa Fluor 488–conjugated anti-rabbit secondary antibody. Scale bars, 20 μm. (D) HeLa cells expressing ATP11A, ATP11B, ATP11C, or their chimeras were grouped into two categories: cells in which the protein was localized to the plasma membrane (PM), and cells in which the protein was localized to the plasma membrane and endosomes (PM + endosomes). In each sample, 236–324 cells were counted. Graphs display the average ± SD of three independent experiments.

at the plasma membrane, some localized to intracellular compartments (Figure 6C, c–c‴). Notably, Lyn_{11}-EGFP-ATP10B-NT colocalized with Lamp-1 but not EEA1 and TfnR (Figure 6E). Moreover, Lyn_{11}-EGFP-ATP11B-NT colocalized with EEA1 and TfnR but not Lamp-1 (Figure 6F). These results strongly suggest that the N-terminus of ATP10B and the C-terminus of ATP11B are critical and sufficient to determine the specific endosomal localization of ATP10B and ATP11B, and likely contain endosomal targeting signals.

Two leucine residues in ATP10B-NT are critical for intracellular trafficking

Given that Lyn_{11}-EGFP-FRB is targeted to the plasma membrane, Lyn_{11}-EGFP-ATP10B-NT and Lyn_{11}-EGFP–ATP11B-CT could be endocytosed soon after targeting to the plasma membrane. Interestingly, we noted that the ETTPLL sequence in the ATP10B-NT is similar to the dileucine motif ([DE]XXXL[LI]; Figure 7A). The dileucine sorting motif plays a critical role in the intracellular trafficking of many transmembrane proteins (Bonifacino and Traub, 2003). To examine whether the ETTPLL sequence of ATP10B-NT serves as the sorting motif, Glu26, Leu30, or Leu31 of ATP10B-NT was replaced with Ala. The constructs were then fused to Lyn_{11}-EGFP, and their subcellular localization was observed. In contrast to the late endosomal localization of Lyn_{11}-EGFP–fused WT ATP10B-NT (Figure 7B, a–a‴), the L30A and L31A mutants of ATP10B-NT largely remained at the plasma membrane (Figure 7B, c–d‴ and f–g‴), suggesting that the two leucine residues are important for the endosomal localization of ATP10B-NT. On the other hand, the E26A mutation did not affect the late endosomal localization of ATP10B-NT (Figure 7B, b–b‴ and e–e‴), indicating that Glu26 is dispensable for the endosomal localization. Although the L30A and L31A mutants primarily localized to the plasma membrane, a small amount of the L31A mutant was detected in endosomal compartments (Figure 7B, d–d‴ and g–g‴). The intracellular puncta of the L31A mutant colocalized with not only Lamp-1 (Figure 7B, d–d‴) but also EEA1 (Figure 7B, g–g‴). Therefore, L30A mutation prevents the endocytosis of ATP10B-NT, and the L31A mutation partially inhibits the endocytosis and targeting to the late endosomal compartments. Taken together, these results suggest that the endosomal localization of Lyn_{11}-EGFP-ATP10B-NT probably results from endocytosis soon after targeting to the plasma membrane, and the two leucine residues are critical for this process.

We next observed the cellular localization of the full length of ATP10B including its point mutants (Figure 8). Unlike ATP10B(WT), the L30A mutant mostly localized to the plasma membrane and L31A mutant partially localized to the plasma membrane (Figure 8A, c–d‴). The E26A mutant mainly localized to late endosomes (Figure 8B, b–b‴), like ATP10B(WT), and some proportion of L31A mutant was observed in late endosomes (Figure 8B, d–d‴) but not in early endosomes (Figure 8C, d–d‴). These results suggest that the two

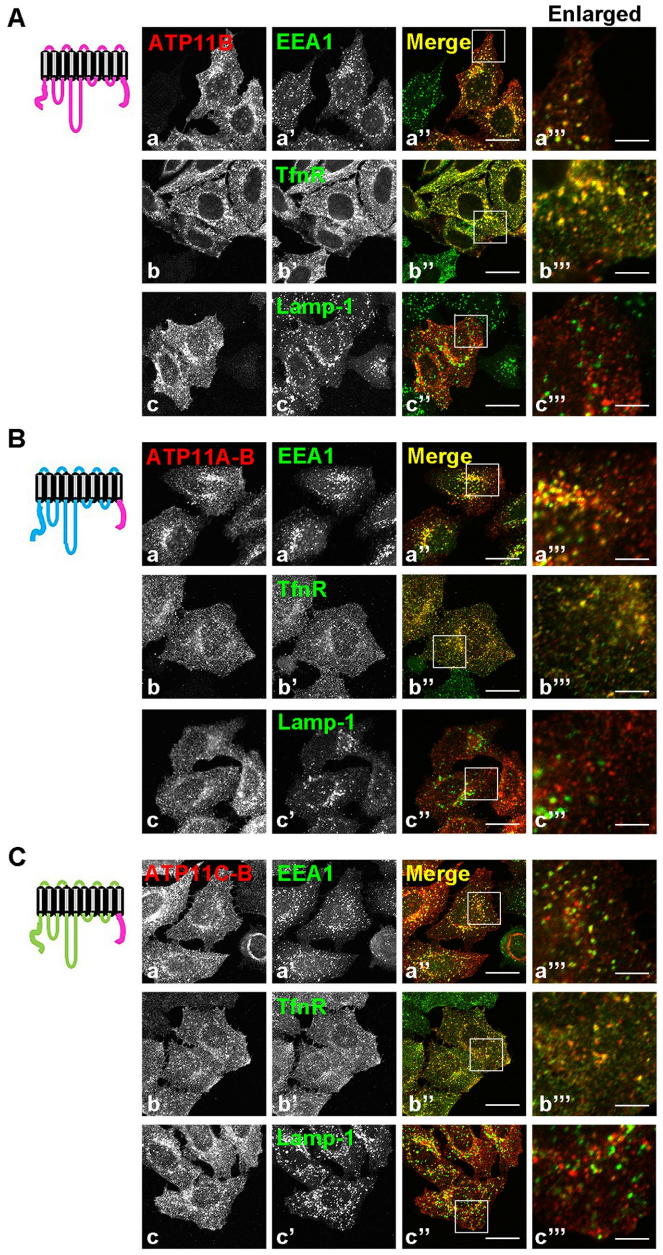

FIGURE 5: Endosomal localization of the C-terminus–swapped ATP11 chimeras. (A–C) HeLa cells transiently coexpressing N-terminally FLAG-tagged CDC50A and C-terminally HA-tagged ATP11B, ATP11A-B, or ATP11C-B were fixed and stained for HA and EEA1 (a marker for early endosomes), TfnR (transferrin receptor, a marker for early/recycling endosomes), or Lamp-1 (marker for late endosomes) followed by incubation with Cy3-conjugated anti-rat antibody and Alexa Fluor 488–conjugated anti-mouse secondary antibody. The images were taken by confocal microscopy. Scale bars, 20 μm. Scale bars in enlarged images, 5 μm.

leucine residues, particularly L30, is critical for the late endosomal localization of ATP10B, which once was delivered to the plasma membrane by recycling pathway in steady state, and/or during the biosynthetic pathway.

DISCUSSION

In this study, we investigated the roles of the N- and C-terminal regions of P4-ATPases with respect to their cellular localization. Importantly, we found that the NT regions of the ATP10 family and the CT regions of the ATP11 family are critical for their cellular localization, suggesting that these cytoplasmic regions include specific membrane-targeting and/or retention signals. Moreover, the N-terminus of ATP10B and the C-terminus of ATP11B serve as endosomal targeting signals for these enzymes. The N-termini of ATP9B and ATP13A2, a P5-ATPase, are required for their Golgi and late endosomal localization, respectively (Takatsu *et al.*, 2011; Holemans *et al.*, 2015). Moreover, the N-termini of ATP9B and ATP13A2 alone are sufficient for their localization through their interactions with the membranes of specific organelles. However, the N-terminus of ATP10B and the C-terminus of ATP11B were not sufficient for targeting to specific endosomal membranes because the N- and C-termini remained distributed in the cytosol when expressed alone (Supplemental Figure S1). By striking contrast, when the plasma membrane–targeting Lyn_{11} sequence was fused to ATP10B-NT or ATP11B-CT, the chimeric constructs became localized to specific endosomal compartments (late endosomes or early/recycling endosomes, respectively) but not to the plasma membrane. Therefore, ATP10B-NT and ATP11B-CT likely serve as intracellular trafficking and targeting signals to direct the proteins from the plasma membrane to specific endosomal compartments. Many transmembrane proteins that localize to intracellular compartments, including Lamp-1, TGN46, and mannose-6-phosphate receptor, cycle between the plasma membrane and endosomes (Dell'Angelica *et al.*, 1999; Ishizaki *et al.*, 2008; Nakai *et al.*, 2013), and ATP11A and ATP11C, which localize to the plasma membrane, also cycle between the plasma membrane and endosomes (Steinberg *et al.*, 2013; Takatsu *et al.*, 2017). The cell surface expression of ATP11A and ATP11C is reduced in SNX27- or VPS35-depleted cells (Steinberg *et al.*, 2013). Thus, SNX27 and the retromer complex regulate the recycling of ATP11A and ATP11C from endosomes to the plasma membrane. Taken together, these data suggest that ATP10B and ATP11B traffic between intracellular compartments and the plasma membrane, and they possess an endosomal targeting and/or retention signal within their NT and CT regions, respectively.

As the NT sequences are diverse among the ATP10 proteins, these regions may play specific roles in individual proteins (Supplemental Figure S2). Consistent with this, the N-terminus is critical for determining the localization of ATP10A, ATP10B, and ATP10D, and the N-terminus of ATP10B is sufficient for the late endosomal targeting of plasma membrane proteins, including Lyn_{11}-EGFP. In addition, ATP10B-NT contains a dileucine-like ExxxLL motif (Supplemental Figure S2), and indeed the two leucine residues are required for the trafficking of Lyn_{11}-EGFP-ATP10B-NT from the plasma membrane to late endosomes (Figure 7), while the Glu residue seems to be dispensable. The P1B-ATPases, ATP7A and ATP7B, also harbor the dileucine-like intracellular trafficking signals in their CT regions (Greenough *et al.*, 2004; Lalioti *et al.*, 2014). It remains to be elucidated whether ATP10B is transported from the plasma membrane to late endosomes or transported from the Golgi complex directly to endosomes during biosynthesis. Nevertheless, when ATP10B is transported to the plasma membrane, the dileucine motif serves as a trafficking signal for targeting to late endosomes (Figure 8). Notably, although D-ATP10B localized to the plasma membrane, Lyn_{11}-EGFP-ATP10D-NT appeared in some punctate structures within the cytoplasm as well as at the plasma membrane. Therefore, the N-terminus of ATP10D might also contain a signal for endocytosis.

We previously showed that the C-terminal SVRPLL sequence of ATP11C-a serves as a dileucine-like motif when the Ser is phosphorylated by protein kinase C (PKC) α and subsequently down-regulated by endocytosis (Supplemental Figure S3; Takatsu *et al.*, 2017).

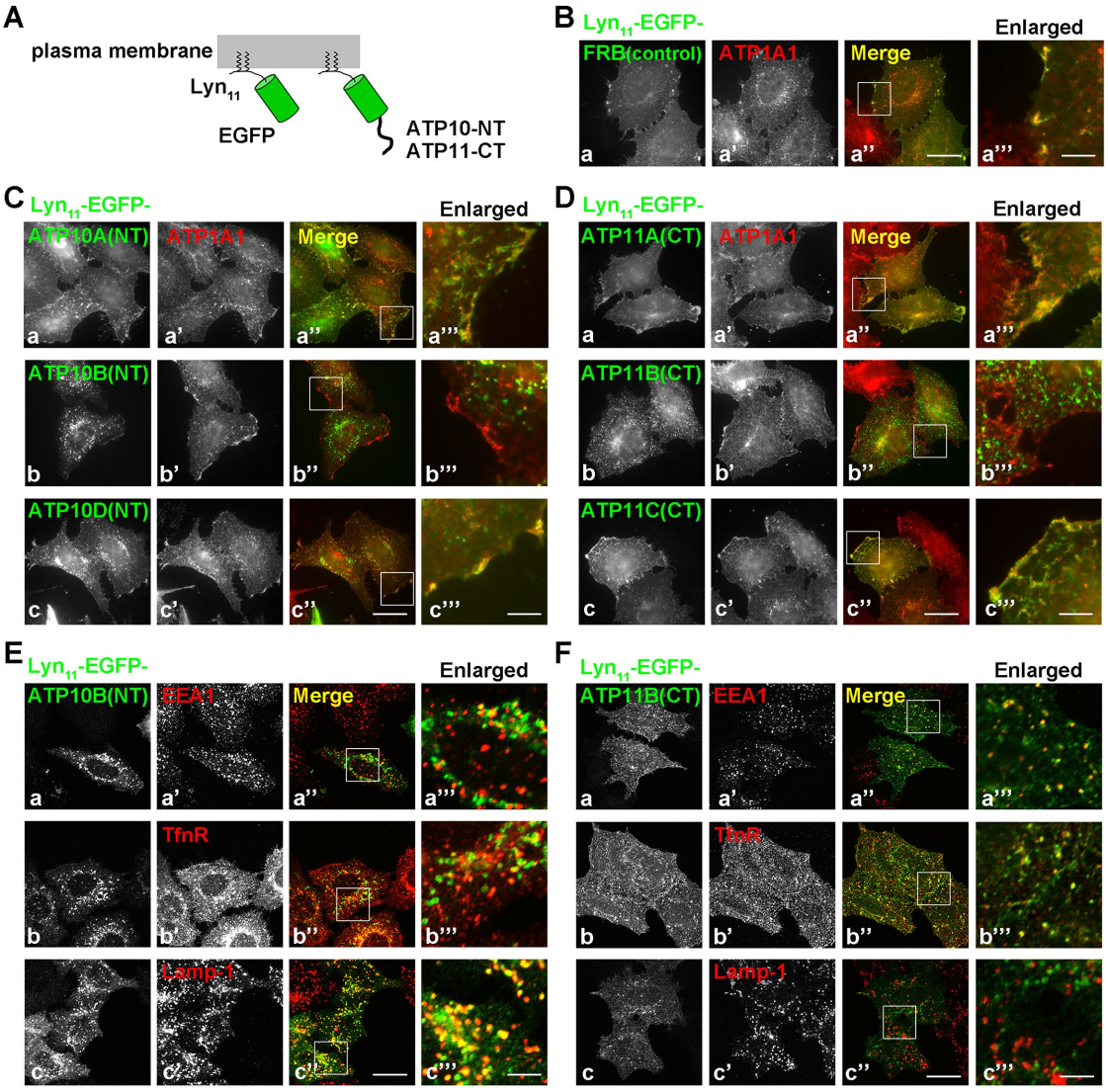

FIGURE 6: The NT regions of ATP10 proteins and the C-terminal regions of ATP11 proteins are sufficient to determine their cellular localization. (A) Schematic representation of chimeric proteins. An EGFP-labeled plasma membrane–targeting signal comprised of the N-terminal 11 amino acids of Lyn (Lyn_{11}) was fused to the N-terminal cytoplasmic region (NT) of each ATP10 protein or the C-terminal cytoplasmic region (CT) of each ATP11 protein. (B–F) HeLa cells were transiently transfected with expression vectors for Lyn_{11}-EGFP–fused ATP10A-NT, ATP10B-NT, ATP10D-NT, ATP11A-CT, ATP11B-CT, or ATP11C-CT (C–F), or the original vector encoding Lyn_{11}-EGFP–fused FRB (FKBP-rapamycin–binding domain) (B). The cells were stained for ATP1A1 (B–D), EEA1, TfnR, or Lamp-1 (E, F) followed by incubation with AlexaFluor 555–conjugated anti-rabbit or anti-mouse secondary antibodies (E, F). Images were taken by confocal microscopy. Scale bars, 20 μm. Scale bars in enlarged images, 5 μm.

Moreover, the C-terminal LLxYKH sequence of ATP11C-b is critical for its polarized localization (Takayama *et al.*, 2019). Therefore, the C-termini of ATP11 proteins play a key role in the regulation of their cellular localization and enzymatic activity at the plasma membrane. Indeed, the C-terminus can determine the localization of ATP11A, ATP11B, and ATP11C (Figure 4), and the C-terminus of ATP11B is sufficient to target plasma membrane proteins, including Lyn_{11}-EGFP, to early/recycling endosomes (Figure 6). Although the endocytic signaling residues of ATP11B-CT are unknown, there might be a signal for trafficking and/or targeting to endosomes.

The C-terminal cytoplasmic region of Drs2p binds to phosphatidylinositol-4-phosphate (PI4P), and this interaction regulates the enzymatic activity of Drs2p. The C-terminus of Drs2p exhibits autoinhibitory activity, and the interaction with PI4P appears to relieve the inhibitory effect (Natarajan *et al.*, 2009; Zhou *et al.*, 2013; Azouaoui *et al.*, 2017;Timcenko *et al.*, 2019). Moreover, the C-terminus of ATP8A2 undergoes phosphorylation that relieves its autoinhibition (Chalat *et al.*, 2017). In addition, the C-terminal GYAFS motif of ATP8A1 binds to the N-domain of ATP8A1 in the E2P state (Hiraizumi *et al.*, 2019). Therefore, the C-terminus seems to be involved in the regulation of the enzymatic activities of these proteins. On the other hand, swapping the N- or C-termini of ATP10 proteins retained their enzymatic activity or substrate specificity (Figure 3), and swapping the C-terminus of ATP11C did not affect its PS/PE-flipping activity (Takatsu *et al.*, 2017). Because there is a great deal of variation among the NT and CT sequences of P4-ATPases (Supplemental Figures S2 and S3), these cytoplasmic regions may play specific regulatory roles with respect to their enzymatic activity and intracellular trafficking.

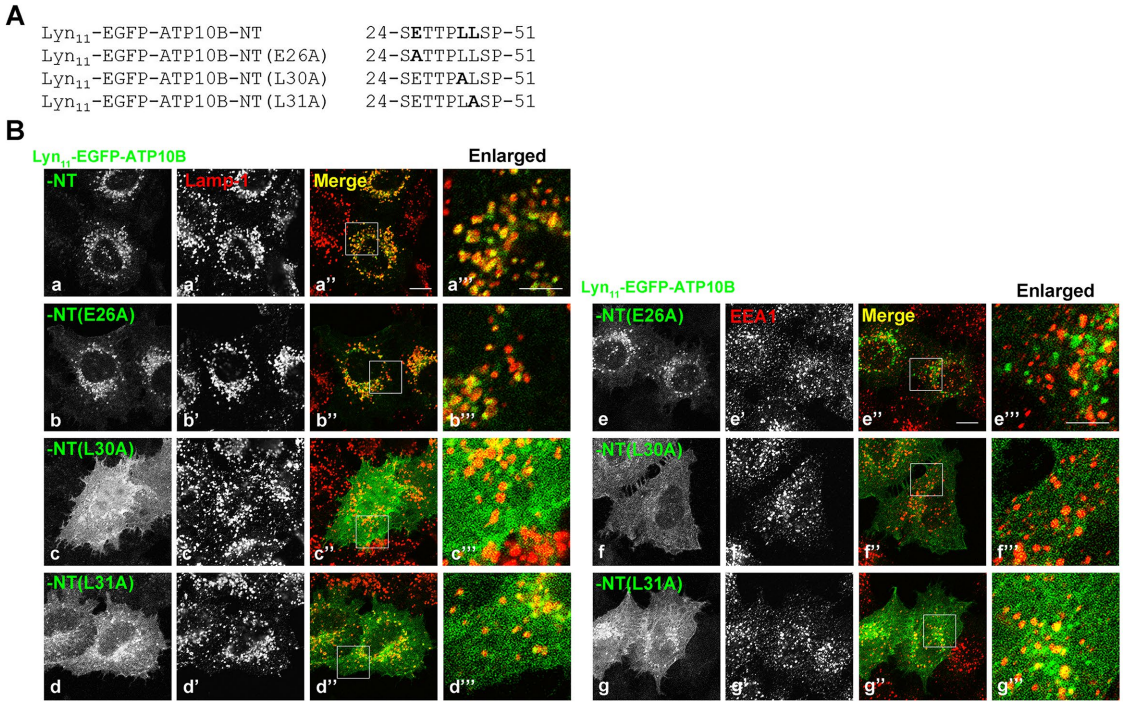

FIGURE 7: Two leucine residues are critical for the endosomal localization of ATP10B-NT. A. Amino acid sequences in the NT cytoplasmic region of human ATP10B and their point mutants were fused to Lyn_{11}-EGFP, as shown in Figure 6A. (B) HeLa cells were transiently transfected with an expression vector for Lyn_{11}-EGFP–fused ATP10B-NT or each mutant. The cells were stained for Lamp-1 (a–d‴) or EEA1 (e–g‴) followed by incubation with an Alexa Fluor 555–conjugated anti-mouse secondary antibody. The images were taken by confocal microscopy. Scale bars, 10 μm. Scale bars in enlarged images, 5 μm.

MATERIALS AND METHODS

Plasmids

Expression vectors for C-terminally HA-tagged human P4-ATPases and N-terminally FLAG-tagged CDC50A were constructed as described previously (Takatsu *et al.*, 2011, 2014). NT- and CT-swapped chimeras of ATP10 proteins and ATP11 proteins were constructed using PCR-based amplification and the seamless ligation cloning extract (SLiCE) cloning method (Zhang *et al.*, 2012). All chimeric constructs were cloned into the pENTR3C vector (Invitrogen/ThermoFisher Scientific) and transferred to the expression vector pCAG-HA using the Gateway system (Invitrogen/ThermoFisher Scientific). The Lyn_{11}-EGFP-FRB construct (Komatsu *et al.*, 2010) was a kind gift from Takanari Inoue (Johns Hopkins University). For construction of Lyn_{11}-EGFP-fused chimeras, DNA fragments encoding the NT regions of ATP10A, ATP10B, or ATP10D, or the C-terminal regions of ATP11A or ATP11B, were amplified by PCR and inserted to replace the FRB using the SLiCE cloning method (Zhang *et al.*, 2012). The Lyn-EGFP–fused C-terminus of ATP11C was constructed as described previously (Takatsu *et al.*, 2017). Point mutations in the N-terminal region of ATP10B were introduced into Lyn_{11}-EGFP-ATP10B-NT using the QuikChange II XL site-directed mutagenesis kit (Agilent Technologies). Point mutations in the full length of ATP10B were introduced into ATP10B(WT) using the QuikChange II XL site-directed mutagenesis kit (Agilent Technologies). All constructs were confirmed by DNA sequencing. All chimeric mutants used in this study are listed in Supplemental Table 1.

Antibodies and reagents

Sources of antibodies used in this study were as follows: monoclonal rabbit anti-ATP1A1 (EP1845Y; Abcam); monoclonal mouse anti-EEA1 and anti-Lamp-1 (BD Biosciences); monoclonal mouse anti-TfnR (Zymed); monoclonal mouse anti-β-tubulin (KMX-1; Millipore); monoclonal mouse anti-DYKDDDDK(1E6) (Wako Chemicals); monoclonal rat anti-HA (3F10; Roche Applied Science); Alexa Fluor–conjugated secondary antibodies (Invitrogen/ThermoFisher Scientific); Cy3-, DyLight-, and horseradish peroxidase–conjugated secondary antibodies (Jackson ImmunoResearch Laboratories). The NBD-labeled lipids (Avanti Polar Lipids) used in this study were NBD-GlcCer (N-[6-[(7-nitro-2-1,3-benzoxadiazol-4-yl)amino]hexanoyl]-D-glucosyl-β1-1′-sphingosine) and NBD-PC (1-oleyl-2-[6-[(7-nitro-2-1,3-benzoxadiazol-4-yl)amino]hexanoyl]-sn-glycero-3-phosphocholine).

Cell culture and immunofluorescence analysis

HeLa cells were cultured in minimal essential medium (Nacalai Tesque) supplemented with 10% heat-inactivated fetal bovine serum at 37°C under a 5% CO_2 atmosphere. HeLa cells were transfected with expression plasmids for CDC50A and ATP10 proteins, ATP11 proteins, or their chimeric constructs using FuGENE6 (Promega), and incubated for 48 h. HeLa cells were transfected with Lyn_{11}-EGFP–fused constructs or HA-tagged ATP10B-NT and ATP11B-CT constructs using FuGENE6 (Promega), and incubated for 24 h. Immunostaining was performed as described previously (Shin *et al.*, 2004; Takatsu *et al.*, 2014) and was visualized using an Axiovert 200MAT microscope (Carl Zeiss) and an A1R-MP confocal laser scanning microscope (Nikon). Briefly, HeLa cells were fixed with 3% paraformaldehyde and then permeabilized with 0.2% saponin for 20 min or 0.1% Triton X-100 for 5 min at room temperature. The cells were blocked with 10% fetal calf serum in phosphate-buffered saline (PBS) at room temperature for 30 min and incubated sequentially with primary and secondary antibodies at room

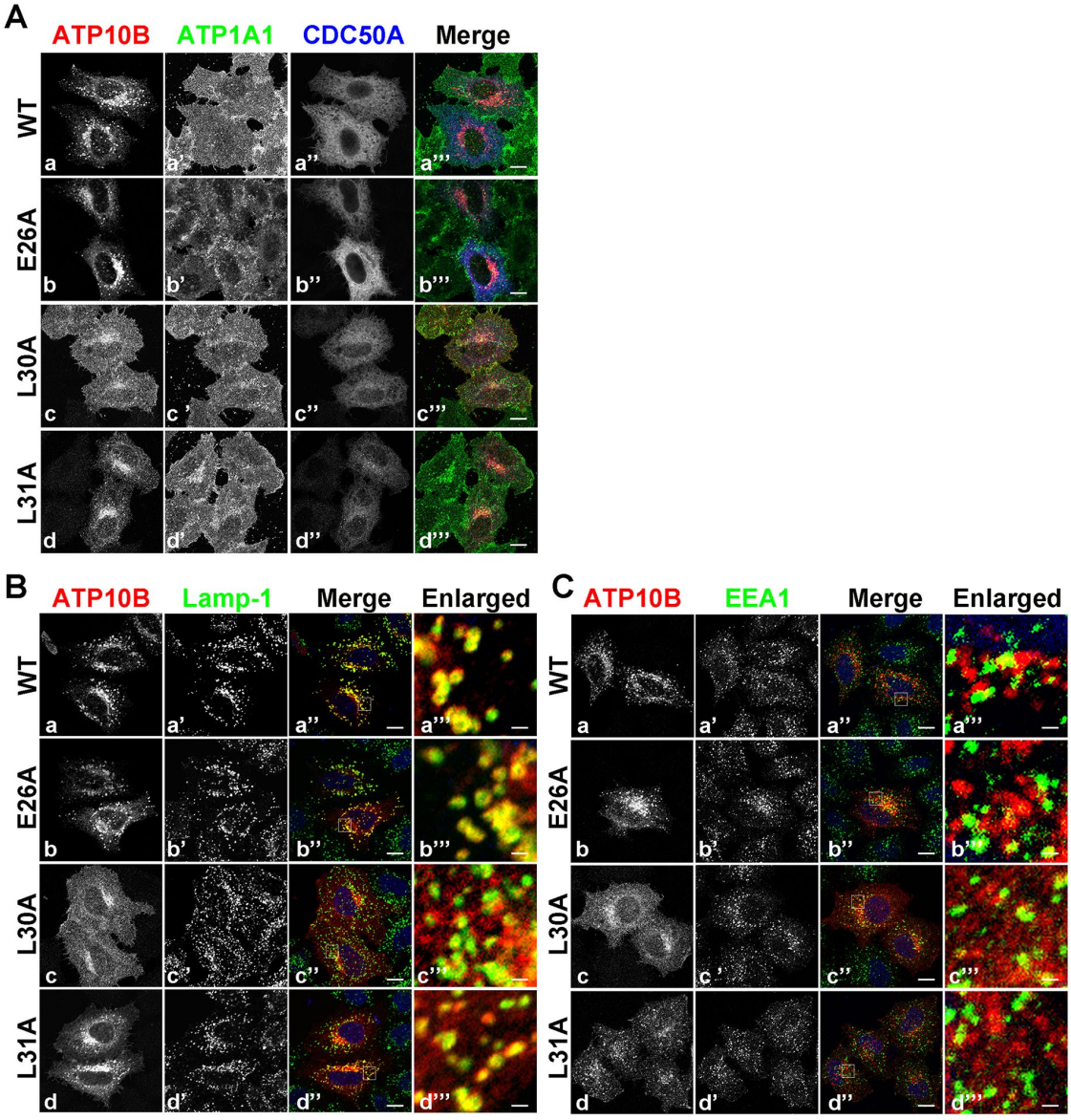

FIGURE 8: Two leucine residues are required for the late endosomal localization of ATP10B. (A–C) HeLa cells were transiently transfected with expression vectors for FLAG-tagged CDC50A and HA-tagged ATP10B(WT), ATP10B(E26A), ATP10B(L30A), or ATP10B(L31A) constructs. The cells were stained for HA, FLAG, and ATP1A1, followed by incubation with Cy3-conjugated anti-rat, Alexa Fluor 488–conjugated anti-mouse, and DyLight649-conjugated anti-rabbit secondary antibodies (A), and stained for HA and Lamp-1 (B), or EEA1 (C) followed by incubation with Cy3-conjugated anti-rat and Alexa Fluor 488–conjugated anti-mouse secondary antibodies, and DAPI (E, F). Images were taken by confocal microscopy. Scale bars, 10 μm. Scale bars in enlarged images, 1 μm.

temperature for 1 h. Coverslips were placed using Mowiol mounting medium.

Flippase assay

Incorporation of NBD-phospholipids was analyzed by flow cytometry as described previously (Takatsu *et al.*, 2014; Roland *et al.*, 2019). In brief, HeLa cells were washed and equilibrated at 15°C for 15 min in 500 μl Hank's balanced salt solution (pH 7.4) containing 1 g/l glucose (HBSS-glucose). The buffer was replaced with 1 μM NBD-labeled lipid in HBSS-glucose, and cells were further incubated at 15°C for 15 min. After incubation, the buffer was replaced with ice-cold PBS containing 2.5% (wt/vol) fatty acid–free bovine serum albumin (BSA; Wako), 5 mM EDTA (EDTA), and 0.5 μg/ml propidium iodide (Nacalai Tesque), and cells were incubated on ice for 30 min. The detached cells (at least 10^4 cells/sample) were analyzed on a FACSCalibur (BD Biosciences) to measure the incorporation of NBD-labeled lipids into the cytoplasmic leaflet of the plasma membrane. Data are expressed as the average ± SD (SD) of at least three independent experiments.

Immunoblotting

HeLa cells were lysed in lysis buffer (20 mM 4-[2-hydroxyethyl]-1-piperazineethanesulfonic acid [HEPES]-KOH, pH 7.4; 150 mM NaCl; 1 mM EDTA; 1% NP-40) containing a protease inhibitor cocktail (Nacalai Tesque) and kept on ice for 30 min. Then, the cell lysates were centrifuged at 16,100 × *g* at 4°C for 30 min in a microcentrifuge to remove insoluble materials. Proteins (30 μg) were separated by SDS–PAGE and electroblotted onto immobilon-P transfer

membranes (Millipore EMD). The membranes were blocked with 5% skimmed milk and sequentially incubated with the indicated primary and horseradish peroxidase–conjugated secondary antibodies. Signals were detected using the Chemi-Lumi One L or Chemi-Lumi One Super kit (Nacalai Tesque).

ACKNOWLEDGMENTS

We thank Takanari Inoue (Johns Hopkins University) for kindly providing Lyn_{11}-EGFP-FRB construct. This work was supported by JSPS KAKENHI Grants no. JP17H03655 (to H.-W.S.) and no. JP17K08270 (to H.T.); the Takeda Science Foundation (to H.-W.S.); and the Naito Foundation (to H.-W.S.).

REFERENCES

Andersen JP, Vestergaard AL, Mikkelsen SA, Mogensen LS, Chalat M, Molday RS (2016). P4-ATPases as phospholipid flippases-structure, function, and enigmas. Front Physiol 7, 275.

Azouaoui H, Montigny C, Dieudonne T, Champeil P, Jacquot A, Vazquez-Ibar JL, Le Marechal P, Ulstrup J, Ash MR, Lyons JA, *et al.* (2017). High phosphatidylinositol 4-phosphate (PI4P)-dependent ATPase activity for the Drs2p-Cdc50p flippase after removal of its N- and C-terminal extensions. J Biol Chem 292, 7954–7970.

Bevers EM, Williamson PL (2016). Getting to the outer leaflet: Physiology of phosphatidylserine exposure at the plasma membrane. Physiol Rev 96, 605–645.

Bonifacino JS, Traub LM (2003). Signals for sorting of transmembrane proteins to endosomes and lysosomes. Annu Rev Biochem 72, 395–447.

Bryde S, Hennrich H, Verhulst PM, Devaux PF, Lenoir G, Holthuis JC (2010). CDC50 proteins are critical components of the human class-1 P4-ATPase transport machinery. J Biol Chem 285, 40562–40572.

Chalat M, Moleschi K, Molday RS (2017). C-terminus of the P4-ATPase ATP8A2 functions in protein folding and regulation of phospholipid flippase activity. Mol Biol Cell 28, 452–462.

Coleman JA, Quazi F, Molday RS (2013). Mammalian P4-ATPases and ABC transporters and their role in phospholipid transport. Biochim Biophys Acta Mol Cell Biol Lipids 1831, 555–574.

Dell'Angelica EC, Shotelersuk V, Aguilar RC, Gahl WA, Bonifacino JS (1999). Altered trafficking of lysosomal proteins in Hermansky-Pudlak syndrome due to mutations in the beta 3A subunit of the AP-3 adaptor. Mol Cell 3, 11–21.

Greenough M, Pase L, Voskoboinik I, Petris MJ, O'Brien AW, Camakaris J (2004). Signals regulating trafficking of Menkes (MNK; ATP7A) copper-translocating P-type ATPase in polarized MDCK cells. Am J Physiol Cell Physiol 287, C1463–C1471.

Hiraizumi M, Yamashita K, Nishizawa T, Nureki O (2019). Cryo-EM structures capture the transport cycle of the P4-ATPase flippase. Science 365, 1149–1155.

Holemans T, Sorensen DM, van Veen S, Martin S, Hermans D, Kemmer GC, Van den Haute C, Baekelandt V, Gunther Pomorski T, Agostinis P, *et al.* (2015). A lipid switch unlocks Parkinson's disease-associated ATP13A2. Proc Natl Acad Sci USA 112, 9040–9045.

Ishizaki R, Shin H-W, Mitsuhashi H, Nakayama K (2008). Redundant roles of BIG2 and BIG1, guanine-nucleotide exchange factors for ADP-ribosylation factors in membrane traffic between the *trans*-Golgi network and endosomes. Mol Biol Cell 19, 2650–2660.

Komatsu T, Kukelyansky I, McCaffery JM, Ueno T, Varela LC, Inoue T (2010). Organelle-specific, rapid induction of molecular activities and membrane tethering. Nat Meth 7, 206–208.

Lalioti V, Hernandez-Tiedra S, Sandoval IV (2014). DKWSLLL, a versatile DXXXLL-type signal with distinct roles in the Cu^{+}-regulated trafficking of ATP7B. Traffic 15, 839–860.

Murate M, Abe M, Kasahara K, Iwabuchi K, Umeda M, Kobayashi T (2015). Transbilayer distribution of lipids at nano scale. J Cell Sci 128, 1627–1638.

Naito T, Takatsu H, Miyano R, Takada N, Nakayama K, Shin HW (2015). Phospholipid flippase ATP10A translocates phosphatidylcholine and is involved in plasma membrane dynamics. J Biol Chem 290, 15004–15017.

Nakai W, Kondo Y, Saitoh A, Naito T, Nakayama K, Shin H-W (2013). ARF1 and ARF4 regulate recycling endosomal morphology and retrograde transport from endosomes to the Golgi apparatus. Mol Biol Cell 24, 2570–2581.

Natarajan P, Liu K, Patil DV, Sciorra VA, Jackson CL, Graham TR (2009). Regulation of a Golgi flippase by phosphoinositides and an ArfGEF. Nat Cell Biol 11, 1421–1426.

Palmgren MG, Nissen P (2011). P-type ATPases. Annu Rev Biophys 40, 243–266.

Palmgren M, Osterberg JT, Nintemann SJ, Poulsen LR, Lopez-Marques RL (2019). Evolution and a revised nomenclature of P4 ATPases, a eukaryotic family of lipid flippases. Biochim Biophys Acta Biomembr 1861, 1135–1151.

Roland BP, Naito T, Best JT, Arnaiz-Yepez C, Takatsu H, Yu RJ, Shin HW, Graham TR (2019). Yeast and human P4-ATPases transport glycosphingolipids using conserved structural motifs. J Biol Chem 294, 1794–1806.

Shin HW, Morinaga N, Noda M, Nakayama K (2004). BIG2, a guanine nucleotide exchange factor for ADP-ribosylation factors: its localization to recycling endosomes and implication in the endosome integrity. Mol Biol Cell 15, 5283–5294.

Shin HW, Takatsu H (2019). Substrates of P4-ATPases: beyond aminophospholipids (phosphatidylserine and phosphatidylethanolamine). FASEB J 33, 3087–3096.

Steinberg F, Gallon M, Winfield M, Thomas EC, Bell AJ, Heesom KJ, Tavaré JM, Cullen PJ (2013). A global analysis of SNX27–retromer assembly and cargo specificity reveals a function in glucose and metal ion transport. Nat Cell Biol 15, 461–471.

Takada N, Naito T, Inoue T, Nakayama K, Takatsu H, Shin HW (2018). Phospholipid-flipping activity of P4-ATPase drives membrane curvature. EMBO J 37, e97705.

Takada N, Takatsu H, Miyano R, Nakayama K, Shin HW (2015). ATP11C mutation is responsible for the defect in phosphatidylserine uptake in UPS-1 cells. J Lipid Res 56, 2151–2157.

Takatsu H, Baba K, Shima T, Umino H, Kato U, Umeda M, Nakayama K, Shin H-W (2011). ATP9B, a P4-ATPase (a putative aminophospholipid translocase), localizes to the *trans*-Golgi network in a CDC50 protein-independent manner. J Biol Chem 286, 38159–38167.

Takatsu H, Takayama M, Naito T, Takada N, Tsumagari K, Ishihama Y, Nakayama K, Shin HW (2017). Phospholipid flippase ATP11C is endocytosed and downregulated following Ca^{2+}-mediated protein kinase C activation. Nat Commun 8, 1423.

Takatsu H, Tanaka G, Segawa K, Suzuki J, Nagata S, Nakayama K, Shin HW (2014). Phospholipid flippase activities and substrate specificities of human type IV P-type ATPases localized to the plasma membrane. J Biol Chem 289, 33543–33556.

Takayama M, Takatsu H, Hamamoto A, Inoue H, Naito T, Nakayama K, Shin HW (2019). The cytoplasmic C-terminal region of the ATP11C variant determines its localization at the polarized plasma membrane. J Cell Sci 132, 231720.

Timcenko M, Lyons JA, Januliene D, Ulstrup JJ, Dieudonne T, Montigny C, Ash MR, Karlsen JL, Boesen T, Kuhlbrandt W, *et al.* (2019). Structure and autoregulation of a P4-ATPase lipid flippase. Nature 571, 366–370.

Tone T, Nakayama K, Takatsu H, Shin HW (2020). ATPase reaction cycle of P4-ATPases affects their transport from the endoplasmic reticulum. FEBS Lett 594, 412–423.

van der Velden LM, Wichers CGK, van Breevoort AED, Coleman JA, Molday RS, Berger R, Klomp LWJ, van de Graaf SFJ (2010). Heteromeric interactions required for abundance and subcellular localization of human CDC50 proteins and class 1 P4-ATPases. J Biol Chem 285, 40088–40096.

Wang J, Molday LL, Hii T, Coleman JA, Wen T, Andersen JP, Molday RS (2018). Proteomic analysis and functional characterization of P4-ATPase phospholipid flippases from murine tissues. Sci Rep 8, 10795.

Zhang Y, Werling U, Edelmann W (2012). SLiCE: a novel bacterial cell extract-based DNA cloning method. Nucleic Acids Res 40, e55.

Zhou X, Sebastian TT, Graham TR (2013). Auto-inhibition of Drs2p, a yeast phospholipid flippase, by its carboxyl-terminal tail. J Biol Chem 288, 31807–31815.